Random Access Compressed Sensing over Fading and Noisy Communication Channels

Fatemeh Fazel, Maryam Fazel and Milica Stojanovic

Abstract

Random Access Compressed Sensing (RACS) is an efficient method for data gathering from a network of distributed sensors with limited resources. RACS relies on integrating random sensing with the communication architecture, and achieves overall efficiency in terms of the energy per bit of information successfully delivered. To address realistic deployment conditions, we consider data gathering over a fading and noisy communication channel. We provide a framework for system design under various fading conditions, and quantify the bandwidth and energy requirements of RACS in fading. We show that for most practical values of the signal to noise ratio, energy utilization is higher in a fading channel than it is in a non-fading channel, while the minimum required bandwidth is lower. Finally, we demonstrate the savings in the overall energy and the bandwidth requirements of RACS compared to a conventional TDMA scheme. We show that considerable gains in energy -on the order of 10 dB- are achievable, as well as a reduction in the required bandwidth, e.g., 2.5-fold decrease in the bandwidth for a network of 4000 nodes.

Index Terms

Wireless Network, Random Access, Compressed Sensing, Fading, Rayleigh, Ricean, Log-normal Shadowing.

I. INTRODUCTION

Wireless sensor network technology has enabled affordable large coverage and long term monitoring of the natural environment [1] such as ocean observation [2], monitoring volcanic eruptions [3] and long term studies of the glaciers [4] which help our understanding of the climate change. Such applications require the least control and intervention as well as minimum energy consumption. The data from distributed sensors is conveyed to a fusion center (FC) where a full map of the sensing field is reconstructed. Once the network is deployed, there can be little access to the sensors, hence re-charging the batteries is difficult. This is especially of concern in underwater networks, where sensor nodes are hundreds of meters below the surface, or in hostile environments where access to the sensor nodes is prohibited. Data

gathering is further exacerbated in situations where bandwidth is constrained and the communication channel introduces distortion. Long term deployment of sensor networks in such environments calls for the integration between sensing, communication, and field recovery.

In [5], [6] we proposed an integrated sensing and communication architecture referred to as *Random Access Compressed Sensing* (RACS), which achieves overall efficiency in terms of the energy per bit of information successfully delivered to the FC. Considering the fact that most natural phenomena have a sparse representation in an appropriate domain, RACS capitalizes on integrating compressed sensing with random channel access. The former supports transmission of sensor data from only a random subset of all the nodes, thus reducing the overall energy consumption, while the latter supports a robust and simple implementation that eliminates the need for synchronization, scheduling, and downlink feedback. In the present paper, we address realistic deployment conditions, that include fading and noisy communication channels. We provide network design principles for such channels, and analyze the network performance in terms of the energy and bandwidth required for successful field recovery.

The rest of the paper is organized as follows. In Section II, we provide an overview of the principles of RACS. In Section III, we study successful packet detection in the presence of channel fading and communication noise and in Section IV, we evaluate system performance under Ricean, Rayligh and Lognormal fading conditions. Section V outlines the design methodology. In Section VI, we study the bandwidth and energy utilization of the network. Finally, we provide concluding remarks in Section VII.

II. RACS: RANDOM ACCESS COMPRESSED SENSING

The theory of compressed sensing [7], [8] establishes that if a signal of dimension N has an S-sparse representation in an appropriate domain $\mathbf{\Psi}$ (referred to as the sparsity basis), it can be recovered, with very high probability, from $\mathcal{O}(\nu S \log N)$ random measurements obtained in a sensing domain $\mathbf{\Phi}$.[1] Consider a sensor network where $N = IJ$ sensors are placed on a grid, with J and I sensors in x and y directions, respectively. At time t, the sensor node located at coordinate (i, j) acquires a measurement $u_{ij}(t)$. This process has a coherence time T_{coh}, such that $u_{ij}(t_1) \approx u_{ij}(t_2)$ for $|t_1 - t_2| \leq T_{coh}$. In what follows we focus on an observation window of size $T \leq T_{coh}$, dropping the time index from the sensor measurements. The measurements are sent to the FC, where the gathered data are used to build a map of the sensing

---

[1]The coefficient ν represents the coherence between the sparsity basis $\mathbf{\Psi}$ and the sensing basis $\mathbf{\Phi}$ and is defined as [9]

$$\nu(\mathbf{\Phi}, \mathbf{\Psi}) = \sqrt{N} \max_{1 \leq k,j \leq N} |\langle \mathbf{\Phi}_k, \mathbf{\Psi}_j \rangle| \tag{1}$$

field (e.g., a geographical, chemical, or a temperature map), denoted by

$$\mathbf{U} = [u_{ij}]_{\substack{i=1,\dots,I \\ j=1,\dots,J}} \tag{2}$$

Many natural signals have a compressible (sparse) representation in the frequency domain,[2] i.e., assuming $\mathbf{u} = \mathrm{vec}(\mathbf{U})$, the vector $\mathbf{v} = \boldsymbol{\Psi}^{-1}\mathbf{u}$ is sparse, where $\boldsymbol{\Psi}^{-1}$ represents the DFT transform matrix.[3] Noting that the spatial coordinate basis and the spatial frequency basis are maximally incoherent,[4] the conditions for compressed sensing hold.

RACS thus works as follows: The sensor node at coordinate (i,j) on the grid measures the signal of interest u_{ij} at random time instants within T_{coh}, independently of the other nodes, at a rate of λ_1 measurements per second. It then encodes each measurement along with the node's location tag into a packet of L bits, which is then modulated and transmitted to the FC in a random access fashion. Because of the random nature of channel access, packets from different nodes may create interference at the FC, or they may be distorted because of noise. A packet is declared erroneous if it does not pass the cyclic redundancy check (CRC) or a similar verification procedure. Motivated by the compressed sensing principle, the key idea in RACS is to let the FC simply discard the erroneous packets, since the FC does not care *which* specific sensors are selected as long as (i) the selected subset is chosen uniformly at random, and (ii) there are sufficiently many useful packets remaining to allow for the reconstruction of the field.

The FC thus discards the packets that are erroneous and collects the remaining useful packets over an observation interval T. The interval T is assumed to be shorter than T_{coh}, such that the process can be approximated as fixed during one such interval. By the end of the observation interval, the useful data at the FC can be expressed as

$$\mathbf{y} = \mathbf{R}\mathbf{u} + \mathbf{z} \tag{5}$$

---

[2]In some cases there may exist bases other than the Fourier, in which the natural signal has an even sparser representation. Without loss of generality, here we will focus on sparse Fourier representations, while providing a general setup encompassing any appropriate basis.

[3]Let $\mathbf{V} = \mathbf{W}_I\mathbf{U}\mathbf{W}_J$ represent the two-dimensional spatial discrete Fourier transform of $\mathbf{U}$, where $\mathbf{W}_I$ is the matrix of discrete Fourier transform coefficients, $\mathbf{W}_I[m,k] = e^{-j2\pi mk/I}$. It can be shown that

$$\mathbf{v} = (\mathbf{W}_J \otimes \mathbf{W}_I)\mathbf{u} \tag{3}$$

where $\mathbf{v} = \mathrm{vec}(\mathbf{V})$. By noting that $\boldsymbol{\Psi} = (\mathbf{W}_J \otimes \mathbf{W}_I)^{-1}$, it follows that

$$\mathbf{v} = \boldsymbol{\Psi}^{-1}\mathbf{u}. \tag{4}$$

[4]The coherence between the (spatial) Fourier domain $\boldsymbol{\Psi}$ and the spatial domain $\boldsymbol{\Phi}$ is $\nu(\boldsymbol{\Psi}, \boldsymbol{\Phi}) = 1$ (see [9]).

where $\mathbf{z}$ represents the sensing noise and $\mathbf{R}$ models the selection of the correct packets. Specifically, $\mathbf{R}$ is a $K \times N$ matrix with K corresponding to the number of useful measurements collected during T. The rows of the matrix $\mathbf{R}$ can be regarded as K rows of an $N \times N$ identity matrix, picked uniformly at random. The FC can form $\mathbf{R}$ from the correctly received packets, since they carry the location tag.

We emphasize the distinction between the *sensing noise* $\mathbf{z}$, which arises due to the limitations in the sensing devices, and the *communication noise*, which is a characteristic of the transmission system. The sensing noise appears as an additive term in Eq. (5), whereas the communication noise results in packet errors and its effect is captured in the matrix $\mathbf{R}$. In addition to communication noise, fading also affects packet detection and similarly affects the matrix $\mathbf{R}$, as will be discussed in Section III.

Noting that $\mathbf{u} = \mathbf{\Psi v}$, where $\mathbf{\Psi}$ is the inverse Discrete Fourier Transform matrix, Eq. (5) can be re-written in terms of the sparse vector $\mathbf{v}$ as

$$\mathbf{y} = \mathbf{R\Psi v} + \mathbf{z} \tag{6}$$

Ignoring the sensing noise $\mathbf{z}$, in order to reconstruct the map of the field, the FC recovers $\mathbf{v}$ by solving the following minimization problem:

$$\text{minimize}_{\tilde{\mathbf{v}}} \ \|\tilde{\mathbf{v}}\|_{\ell_1} \quad \text{subject to} \ \mathbf{R\Psi}\tilde{\mathbf{v}} = \mathbf{y}. \tag{7}$$

The theory of compressed sensing (specifically, [7]) states that as long as the number of observations, picked uniformly at random, is greater than $N_s = CS \log N$, then with very high probability the solution to the convex optimization problem (7) is unique and is equal to $\mathbf{v}$. Thus, it suffices to ensure that the FC collects a minimum number of packets, $N_s = CS \log N$, picked uniformly at random from different sensors, to guarantee accurate reconstruction of the field with very high probability. Note that C is a constant that is independent of S and N.[5]

Note that the results in this paper are not restricted to the grid model and can be extended to the cases where the sensors are either placed on a nonuniform rectangular grid, or placed non-uniformly on parallel lines. In such scenarios, the Fourier representation is replaced by the two-dimensional nonuniform discrete Fourier transform [10]. Subsequently, as shown in [11] recovery is achieved using (7).

---

[5]If the signal has a sparse representation in a basis $\mathbf{\Psi}'$ other than the Fourier basis, RACS is still applicable with the condition that the number of required measurements is now adjusted to $N_s = C\nu^2(\mathbf{\Phi}, \mathbf{\Psi}')S \log N$ where $\mathbf{\Phi}$ is the spatial domain.

III. Packet Detection in Fading and Noise

A wireless communication channel is typically modeled by a distance-dependent propagation loss, shadowing, and small-scale fading. Let $L(d_i)$ represent the attenuation or path loss, which depends on the distance d_i between the sensor generating packet i and the FC. Since the network is stationary, each node can be equipped with the knowledge of its distance to the FC, which remains unchanged throughout the data collection interval. Each node can thus compensate for the path loss $L(d_i)$ by adjusting its transmission power. This ensures that the packets from all the nodes arrive at the FC at the same nominal power P_0. The total channel gain c_i, observed by the i-th packet, is thus modeled as

$$c_i = e^{g_i} h_i \tag{8}$$

where $g_i \sim \mathcal{N}(0, \sigma_g^2)$ models the large-scale lognormal shadowing and $h_i \sim \mathcal{CN}(\overline{h}, \sigma_h^2)$ models the small-scale fading. We assume a quasi-static fading model in which the channel coefficient c_i is fixed for the duration of a packet T_p, and changes independently from one packet to the next. This is a reasonable assumption since the packets generated by a single node are transmitted at a relatively low rate, i.e., they are distanced sufficiently apart in time such that they undergo independent fades. We also assume that the colliding packets undergo uncorrelated channels. This is a fair assumption because the colliding packets are not likely to be from neighboring nodes.

In the absence of channel fading and communication noise, packet loss in RACS is caused by collisions, i.e., an overlap in the arrival time of two packets, which results in the loss of both packets [5], [12]. When fading is present, the situation is somewhat changed since not every collision has to result in packet loss. Namely, it is possible that although two (or more) packets overlap at the FC, one is sufficiently stronger so that it can be successfully detected. Below we discuss the probability of successful reception.

A. Interference Model

The received signal at the FC is given by

$$v_n(t) = c_0 u_0(t) + i_n(t) + w(t) \tag{9}$$

where $u_0(t)$ is the desired signal, $i_n(t)$ is the interference and $w(t)$ is the additive white Gaussian noise with power N_0B, where B is the bandwidth. The interfering term can be expressed as

$$i_n(t) = \sum_{i=1}^{n} c_i u_i(t - \tau_i) \tag{10}$$

where $u_i(t)$ is the i-th interferer's signal, τ_i is the difference in the arrival times of the interfering signal with respect to the signal of interest, and the number of interfering packets n is a random variable with probability distribution $P(n)$. Assuming that packet arrivals follow a Poisson distribution, we have that

$$P(n) = \frac{(2N\lambda_1 T_p)^n}{n!} e^{-2N\lambda_1 T_p} \tag{11}$$

where $T_p = L/B$ is the packet duration.[6]

For a given node, let $X_0 = |c_0|^2 P_0$ represent the power of the desired packet, and I_n represent the total interference power. We assume that X_0 and I_n follow the probability distributions f_X and f_I, respectively. The instantaneous signal to interference and noise ratio (SINR) is given by

$$\gamma = \frac{X_0}{I_n + N_0 B} \tag{12}$$

In the worst case scenario, the packet arrivals are synchronous, i.e., $\tau_i = 0$ for $i \in \{1, \ldots, N\}$. The interference power is then given by $I_n = \sum_{i=1}^{n} |c_i|^2 P_0 = Y_n$, which follows a probability distribution f_Y. This situation, however, represents a pessimistic scenario since packet transmissions in RACS are not synchronized. Rather than considering various scenarios for the overlapping of packets, we employ a simplified model in which we assume that the strongest interferer dominates the term $i_n(t)$ [13], i.e., we assume that the interference power is $I_n = max_{i \in \{1, \ldots, n\}} |c_i|^2 P_0 = M_n$, which has a probability distribution f_M. Specifically,

$$f_M(z) = n F_X(z)^{n-1} f_X(z) \tag{13}$$

where $F_X(x)$ is the cumulative distribution function of X_0.

Thus we have two methods to model the interfering power,

$$I_n = \begin{cases} Y_n = \sum_{i=1}^{n} |c_i|^2 P_0 & \text{(model a)} \\ M_n = \max_i |c_i|^2 P_0 & \text{(model b)} \end{cases} \tag{14}$$

---

[6]Throughout this paper we use bandwidth and bit rate interchangeably.

Model (a) assumes the worst case scenario, leading to an overestimation of the effect of interference and thus slightly pessimistic results for the probability of successful reception. In contrast, model (b) underestimates the effect of the interference, resulting in a probability of success that is slightly greater than the one predicted using model (a). The models (a) and (b) given by (14) thus provide upper and lower bounds, respectively, on the actual interfering power.

B. Probability of Successful Reception: Outage Model

For a given number of interfering packets n, we employ the outage model to describe the probability of successful reception $p_{s|n}(\gamma)$. In this model, $p_{s|n}(\gamma)$ is described by a step function as

$$
p_{s|n}(\gamma) = \begin{cases} 0, & \gamma < b \\ 1, & \gamma \geq b \end{cases} \tag{15}
$$

The effects of coding, modulation and other system parameters are implicit in one parameter $b > 1$,[7] which is a predefined threshold with a typical value $b = 2 - 6$ [14], [15].[8]

Under the outage model, averaging $p_{s|n}(\gamma)$ over the fading statistics results in (see Appendix A)

$$
p_{s|n} = \begin{cases} \int_{bN_0B}^{\infty} f_X(x)dx & \text{for } n = 0 \\ \int_b^{\infty} \int_{N_0B}^{\infty} f_X(\gamma w) f_I(w - N_0B)w\,dw\,d\gamma & \text{for } n \geq 1 \end{cases} \tag{17}
$$

where $f_I = f_Y$ for model (a) and $f_I = f_M$ for model (b). The total probability of successful reception is then given by

$$
p_s = \sum_{n=0}^{N} P(n)p_{s|n} \tag{18}
$$

Small-scale fading, modeled by h_i in Eq. (8), creates relatively fast variations in the channel, and is thus responsible for short term signal variations. Shadowing, on the other hand, occurs over longer time scales, creating slow variations in the mean signal amplitude. Several different models for the probability distribution of a composite multipath/shadowed environment have been proposed, among which are the composite Gamma/lognormal and the Suzuki models [17], [18]. In most environments, however, either

---

[7]Note that if multi-user detection techniques are employed, the value of b may be smaller than 1. In this paper we assume a single-user detector.

[8]As an alternative to the outage model, we can use the BER model. Treating interference as Gaussian noise, we can use the bit error probability $p_b(\gamma)$ to determine the probability of receiving a correct packet as

$$
p_{s|n}(\gamma) = (1 - p_b(\gamma))^L \tag{16}
$$

Using powerful long codes, Eq. (16) approaches a step function, thus $p_{s|n}(\gamma)$ in the BER model approaches that in the outage model [16].

shadowing or multipath fading is the dominant factor. In what follows, we proceed to investigate the probability of successful reception under Ricean, Rayleigh and log-normal fading statistics.

IV. FADING SCENARIOS

A. Small-scale Fading: Ricean and Rayleigh models

In propagation environments where the data collection interval T is short compared to the de-correlation interval of the shadowing, the variation in shadowing can be assumed negligible. The effects of path loss and shadowing, included in a gain $G_i = L(d_i)e^{g_i}$, can thus be pre-compensated at the transmitter by means of a power control mechanism, i.e., the transmitter adjusts its power to P_0/G_i^2. The power control can be achieved by an occasional downlink beacon which enables the sensor node to estimate the shadowing coefficient. Thus, only small scale fading remains in model (8).

The distribution of the amplitude of the channel $R_i = |h_i|$ in Ricean fading is given by

$$f_{R_i}(r_i) = 2(K+1)r_i \exp\left(-r_i^2(K+1) - K\right) I_0\left(2\sqrt{K(K+1)}r_i\right) \tag{19}$$

where K is the Ricean factor (defined as the ratio of the power in the specular component to the power in the scattered component), where we assume that the sum power in both components is normalized to one, and $I_0(\cdot)$ is the zero-order modified Bessel function of the first kind. In a Ricean fading channel, the probability of successful reception, given by Eq. (17), can be evaluated numerically using the distributions $f_X(x)$, $f_Y(y)$ and $f_M(z)$ provided in the Appendix B.

In the special case when there is no LOS component present, i.e., when $K = 0$, the envelope of h_i follows a Rayleigh distribution. In this case,

$$f_X(x) = \frac{1}{P_0}e^{-x/P_0} \tag{20}$$

For the interference model (a) we have that

$$f_Y(y) = \frac{1}{P_0}\frac{(y/P_0)^{n-1}}{(n-1)!}e^{-y/P_0} \tag{21}$$

and for the interference model (b) we have that

$$f_M(z) = \frac{n}{P_0}\left(1 - e^{-z/P_0}\right)^{n-1} e^{-z/P_0} \tag{22}$$

Defining $\gamma_0 = P_0/N_0 B$, the probability of successful reception is obtained in closed form as

$$p_s = e^{-b/\gamma_0} e^{-2N\lambda_1 T_p \frac{b}{1+b}} \tag{23}$$

and

$$p_s = e^{-b/\gamma_0} e^{-2N\lambda_1 T_p} \left(1 + \sum_{n=1}^{N-1} \frac{(2N\lambda_1 T_p)^n}{n!} \sum_{i=0}^{n} \binom{n}{i} \frac{(-1)^i}{1+i/b} \right) \tag{24}$$

for models (a) and (b), respectively. In a non-fading channel, provided that $\gamma_0 \geq b$, p_s corresponds to the probability of no collision [5]. Also, in a noiseless fading channel, the probability of successful reception reduces to $p_s = e^{-2N\lambda_1 T_p \frac{b}{b+1}}$ [19].

1) Numerical Examples: We now provide numerical results to demonstrate the impact of small scale fading on the probability of successful reception. Unless otherwise noted, we employ the following system parameters in our numerical examples: $N = 2500$ nodes, $L = 1000$ bits per packet, $\lambda_1 = 10^{-3}$ packet/sec and $b = 4$.

Fig. 1 shows the probability of successful reception in Rayleigh fading ($K = 0$) using the two models (a) and (b) for interference given by Eqs. (23) and (24), respectively. As expected, model (b) predicts a larger p_s than model (a). We note that for our choice of system parameters, the bounds on p_s, provided by models (a) and (b), are tight, and the gap further diminishes as bandwidth is increased. Thus, the actual p_s is approximated relatively accurately by each model. Throughout the rest of the paper, unless otherwise noted, we use model (a) and design the system for the worst case scenario, keeping in mind that the actual system performance will be slightly better than assumed by this model.

Fig. 2 shows p_s in a Ricean fading channel for $K = 3$ and $K = 6$ dB as well as in a Rayleigh fading channel. In a non-fading channel, when $\gamma_0 < b$, due to the high noise level, packets are not successfully detected. We observe that fading enhances the probability of successful reception in two regimes: 1) when noise is dominant (i.e., when γ_0 is small), meaning that most packet losses are caused by noise, and 2) when noise is small and interference is dominant, i.e., most packet losses are due to collisions. In both cases, fading boosts the performance by turning some instances of packet loss into successful receptions. In other scenarios, fading deteriorates the performance.

Finally, Fig. 3 shows p_s versus the Rice factor K. We have considered two scenarios: Fig. 3(a) shows p_s for $\gamma_0 = 15$ dB. In this noise regime, the success rate is lower in fading. Fig. 3(b) shows p_s for $\gamma_0 = 30$ dB. In this scenario, most packet losses are a result of collisions (and not noise), for which

fading enhances the success rate. As expected, the Ricean and Rayleigh fading scenarios converge when $K = 0$, and as K increases, p_s in a Ricean fading channel approaches that in a non-fading channel.

B. Log-normal Shadowing

When the packet duration T_p is long compared to the shadowing time-scale, the receiver can average out the effects of small-scale fading. Thus the communication system performance will only depend on the log-normal shadowing, i.e., the slow variations of the mean signal. It is shown that in an urban land mobile environment, de-correlation of log-normal shadowing occurs on time-intervals on the order of 7-13 seconds [20]. Thus, when T_p is on the order of a few seconds (i.e., when B is small), the small-scale fading can be averaged out. The pdf of the received power of a packet can then be modeled as

$$f_X(x) = \frac{1}{\sqrt{2\pi\sigma^2}x}e^{-(\log x)^2/2\sigma^2} \tag{25}$$

where $\sigma = 2\sigma_g$, with σ_g denoting the standard deviation of g_i in Eq. (8). The dB spread of the channel is defined as $\sigma_{dB} = (0.1\log 10)\sigma$, which, in practice, takes on values between $6 - 12$dB [21]. The pdf of the interference power in model (b) is determined as

$$f_M(z) = nQ\left(\frac{-\log z}{\sigma}\right)^{n-1}\frac{1}{\sqrt{2\pi\sigma^2}z}e^{-(\log z)^2/2\sigma^2} \tag{26}$$

In order to determine the pdf of the interference power in model (a), we note that the sum of log-normal random variables can be approximated as a log-normal, i.e.,

$$f_Y(y) = \frac{1}{\sqrt{2\pi\sigma_n^2}x}e^{-(\log x - m_n)^2/2\sigma_n^2} \tag{27}$$

The parameters m_n and σ_n depend on the number of interfering packets n, and can be approximated using several different methods [22]–[24]. Fig. 4 shows the probability of successful reception under model (b) compared with that under model (a). For model (a) we use the Wilkinson's, the Fenton's, and the Schwartz-Yeh's methods to determine m_n and σ_n. All of these methods rely on approximating the sum to be log-normally distributed, but use different approximation techniques. Although theoretically, model (b) provides an upper-bound on p_s, we note from the figure that the resulting approximate p_s in model (a) surpasses that obtained by model (b). Consequently, the approximations required for model (a) are not of sufficient accuracy to be used in predicting p_s. For our analysis in log-normal shadowing, we thus employ model (b) which does not rely on any approximations.

In [21], [22], Farley proposes an approximation to the CDF of the sum of log-normal random variables, without making any assumption on the distribution of the sum, given by

$$F_Y(y) \approx \left(1 - Q\left(\frac{\log y}{\sigma}\right)\right)^n \qquad (28)$$

It is interesting to note that this expression coincides with the CDF of our model (b),

$$F_Z(z) = \text{Prob}(\max_i X_i \leq z) = (\text{Prob}(X_i \leq z))^n = \left(1 - Q\left(\frac{\log z}{\sigma}\right)\right)^n \qquad (29)$$

where X_i is log-normally distributed according to Eq. (25).

Fig. 5 shows p_s for several values of the dB spread, as well as for the non-fading case, for $B = 5$ kbps. We observe a similar trend to that of Rayleigh and Ricean fading channels. Since the employed bandwidth is smaller than the bandwidth in Fig. 2, packet collisions are more likely to occur, thus fading provides a greater improvement in p_s than in systems with large bandwidths.

V. NETWORK DESIGN PRINCIPLES

A. Arrival of Useful Packets

We assume that each node generates packets according to independent Poisson processes at an average rate of λ_1 packets per second. Among the successfully received packets, there may be more than one packet corresponding to a single node. Considering that the sensing field has not changed, the extra packets, if successfully received, are redundant. The total number of packets that are used in the reconstruction process, referred to as the *useful packets* and denoted by $K(\lambda_1, T)$, is thus the number of received packets left after discarding the erroneous and repetitive packets at the end of the observation interval T. In a given interval, reconstruction will be successful if sufficiently many useful packets are collected. Otherwise, reconstruction for that particular interval will fail. In what follows we determine the probability distribution of the number of useful packets $K(\lambda_1, T)$.

For a particular node, let $\mathcal{N}_1(T)$ denote the number of packets generated during T that are successfully received. Hence, the number of useful (i.e., successfully received non-repeated) packets generated at each node during T is given by

$$M(T) = \begin{cases} 0, & \mathcal{N}_1(T) = 0 \\ 1, & \mathcal{N}_1(T) \geq 1 \end{cases} \qquad (30)$$

The probability of receiving a useful packet from a node is $p_g = \text{Prob}\{M(T) = 1\}$, which can be expressed as

$$p_g = \text{Prob}\{\mathcal{N}_1(T) \geq 1\} = \sum_{l=1}^{m} \frac{(\lambda_1 T)^l}{l!} e^{-\lambda_1 T}[1 - (1 - p_s)^l] \tag{31}$$

where each term in the summation is the product of the probability that the node generates l packets during T, and the probability that one or more of the generated packets are successfully received. Note that since a node does not interfere with its own packet, the maximum number of packets that are generated by a single node during T is given by $m = \lfloor \frac{T}{T_p} \rfloor \gg 1$. With this in mind, the expression (31) is approximated as $p_g = 1 - e^{-p_s \lambda_1 T}$.

From (30), the effective average number of packets received from a given node during T is $\overline{M(T)} = p_g$. The average effective arrival rate of packets at the FC is thus

$$\lambda' = \frac{N p_g}{T} = \frac{N}{T}(1 - e^{-p_s \lambda_1 T}) \tag{32}$$

where p_s is the probability of successful reception for a given node, determined for various fading conditions in Section IV.

The arrival of useful packets then follows a Poisson process with an effective average arrival rate λ' given by Eq. (32). i.e.,

$$\text{Prob}\{K(\lambda_1, T) = k\} = \frac{(\lambda' T)^k}{k!} e^{-\lambda' T} \tag{33}$$

Using this model, we proceed to determine the sensing rate necessary to achieve a desired performance requirement.

B. Probability of Sufficient Sensing

We define the *probability of sufficient sensing* as the probability that the FC collects N_s or more useful packets during T, and we specify the performance requirement as the minimum probability of sufficient sensing, P_s. Thus,

$$\text{Prob}\{K(\lambda_1, T) \geq N_s\} \geq P_s \tag{34}$$

The condition (34) can equivalently be stated as

$$\alpha \geq \alpha_s \tag{35}$$

where $\alpha = \lambda' T$ represents the average number of useful packets collected in T and is given by

$$\alpha = N(1 - e^{-\lambda_1 T p_s}) \tag{36}$$

and α_s is a design target. For a given N_s and a desired P_s, one can find the corresponding α_s numerically from Eq. (34). For example, assuming $N = 2500$ and $S = 20$ ($N_s = 2S \log N = 313$ packets), a required probability of sufficient sensing $P_s = 0.99$ results in $\alpha_s = 355$ packets.

C. Design Objective

The design objective is to determine the per-node sensing rate λ_1 that is necessary to ensure sufficient sensing. The condition (35) implies that

$$\lambda_{1s} \leq \lambda_1 \leq \lambda_{1c} \tag{37}$$

where λ_{1s} and λ_{1c} are the solutions to $\alpha = \alpha_s$. We are only interested in those values of λ_1 for which the system is *stable*, i.e., those values for which increasing λ_1 results in an increased number of useful packets. Thus the desired value of the per-node sensing rate lies in the stable region

$$\lambda_{1s} \leq \lambda_1 \leq \lambda_{1m} \tag{38}$$

where λ_{1m} is the point at which α reaches its maximum value $\alpha_{\max}$, as noted in Fig. 6. The desired operating point is now chosen to be at the lower edge of the stable region, i.e., at the minimum per-node sensing rate λ_{1s}, since a lower per-node sensing rate corresponds to lower energy consumption, as we will discuss in Section VI.

In a Rayleigh fading channel, using Eq. (23), the per-node sensing rate λ_{1s} can be expressed as

$$\lambda_{1s} = \frac{-1}{2NT_p\beta} \cdot W_0 \left(\frac{2NT_p\beta e^{\frac{b}{\gamma_0}}}{T} \log \left(1 - \frac{\alpha_s}{N} \right) \right) \tag{39}$$

where $\beta = b/(b+1)$ and $W_0(\cdot)$ denotes the principal branch of the Lambert W function.[9] In other fading scenarios, λ_{1s} can be determined numerically for a given α_s.

Fig. 7 shows the minimum per-node sensing rate λ_{1s} for Rayleigh, Ricean and non-fading channels. We notice that fading increases the required sensing rate. Note that if a different α_s is required, say because

---

[9]The Lambert W function $W(x)$ satisfies the equation $W(x)e^{W(x)} = x$ for $x \geq -1/e$. The branch satisfying $W(x) \geq -1$ is denoted by $W_0(x)$.

new nodes are introduced into the network, the per-node sensing rate is easily adjusted. Hence, RACS is *scalable*, i.e., it can be tailored to a varying number of nodes.

VI. BANDWIDTH AND ENERGY REQUIREMENTS

A. Bandwidth

To achieve a certain sufficient sensing probability, a minimum bandwidth B_s is required. Let us define

$$x_s = \frac{2NT_p\beta e^{b/\gamma_0}}{T} \log\left(1 - \frac{\alpha_s}{N}\right) \tag{40}$$

In order to have a valid solution for λ_{1s}, Eq. (39) implies that $W_0(x_s)$ has to be negative. Thus

$$-1 \leq W_0(x_s) \leq 0 \tag{41}$$

The limit $W_0(x_s) = 0$ in (41) is achieved when $x_s = 0$, or equivalently, when $B \to \infty$. The other limit, $W(x) = -1$, is achieved when $x_s = -1/e$ which corresponds to the minimum bandwidth. The minimum bandwidth B_s in Rayleigh fading is thus obtained in closed form as

$$B_s = \frac{2NL\beta}{T} \cdot e^{(1+b/\gamma_0)} \cdot \log\left(\frac{1}{1 - \alpha_s/N}\right) \tag{42}$$

In other fading conditions B_s can be determined numerically. Now in the non-fading case, for $\gamma_0 \geq b$ we have that

$$B_{s,\text{no fading}} = \frac{2NL}{T} \cdot e \cdot \log\left(\frac{1}{1 - \alpha_s/N}\right) \tag{43}$$

Depending on the choice of the modulation and coding (i.e., the parameter b) and the average received SNR γ_0, fading can lower the bandwidth requirements of RACS. Specifically in Rayleigh fading, if

$$\gamma_0 \geq \frac{b}{\log\left(\frac{b+1}{b}\right)} \tag{44}$$

we observe a saving in the minimum required bandwidth, given by

$$\frac{B_s}{B_{s,\text{no fading}}} = \beta e^{b/\gamma_0} \tag{45}$$

This can be seen from Fig. 8, which shows the minimum required bandwidth in Rayleigh, Ricean and non-fading channels, plotted versus γ_0, for $\gamma_0 > b/\log\left(\frac{b+1}{b}\right)$.

B. Energy

The total average energy required for one field reconstruction is

$$E = N\lambda_1 T \cdot P_T \cdot T_p \tag{46}$$

where the first term ($N\lambda_1 T$) is the average number of nodes that transmit in one collection interval T and P_T is the average per-node transmission power. Determining the average transmission power P_T over the entire network in general depends on the geometry of the system and the placement of the nodes. When shadowing is pre-compensated at the transmitter,

$$P_T = P_0 E_{d_i}\{L(d_i)^{-2}\} E_g\{e^{-2g}\} = P_0 \Gamma e^{2\sigma_g^2} \tag{47}$$

where $\Gamma = E_{d_i}\{L(d_i)^{-2}\}$ is the path loss averaged over the nodes' distances to the FC. When shadowing is not compensated,

$$P_T = P_0 \Gamma \tag{48}$$

It is worthwhile to note that in order to maintain a fixed received SNR γ_0, the transmission power P_0 has to scale with the bandwidth, i.e., $P_0 = N_0 B \gamma_0$, resulting in

$$P_T = N_0 B \gamma_0 \cdot \eta \tag{49}$$

where $\eta = \Gamma$ or $\eta = \Gamma e^{2\sigma_g^2}$ depending on whether the lognormal component of the channel is compensated at the transmitter.

For a given bandwidth B, the energy consumption in (46) is minimized if one chooses the minimum sensing rate $\lambda_{1s}(B)$, i.e.,

$$E_{\min}(B) = N\lambda_{1s}(B) T N_0 \gamma_0 \eta L \tag{50}$$

where we have substituted for P_T from Eq. (49). For a fixed bandwidth B, Fig. 9 shows the minimum sensing rate λ_{1s} plotted versus γ_0. We observe that for mid-range γ_0 (i.e., $\gamma_0 = 15 - 27$ dB) the required λ_{1s} in Rayleigh fading is larger than that in a non-fading channel, hence energy consumption is higher. For larger γ_0 (i.e., $\gamma_0 > 27$ dB) the required λ_{1s} is lower in fading, consequently, the energy consumption is lower for this range of γ_0.

The energy expenditure $E_{\min}$ in Eq. (50) depends on the transmission bandwidth B through λ_{1s}. We

note that $\lambda_{1s}(B)$ is largest when $B = B_s$ and decreases with B, reaching a limiting value $\lambda_{1s}(\infty)$ as $B \to \infty$. This value is analytically derived as

$$\lambda_{1s}(\infty) = \frac{e^{b/\gamma_0}}{T} \log \frac{1}{1 - \alpha_s/N} \tag{51}$$

The lower and upper bounds on the energy consumption of RACS in Rayleigh fading are thus determined as

$$E_{\text{low}} = \lim_{B \to \infty} E_{\min}(B) = N N_0 \gamma_0 \eta L \cdot e^{b/\gamma_0} \cdot \log \frac{1}{1 - \alpha_s/N} \tag{52}$$

and

$$E_{\text{up}} = E_{\min}(B_s) = N N_0 \gamma_0 \eta L \cdot e^{1+b/\gamma_0} \cdot \log \frac{1}{1 - \alpha_s/N} \tag{53}$$

We note that the lower and upper bounds are within a constant gap of size e.

C. Savings With Respect to a Benchmark Network

To demonstrate the advantage of the RACS scheme, we compare the energy and bandwidth requirements of RACS with those of a conventional (benchmark) design. The benchmark scheme is a TDMA network in which all N nodes transmit using pre-assigned time slots. The bandwidth and energy requirements of a TDMA network over an ideal communication channel (i.e., no channel fading or noise) are given by [5]

$$B_{s,TDMA} = \frac{NL}{T} \tag{54}$$

and

$$E_{TDMA} = N T_p P_T = N N_0 \gamma_0 \eta L \tag{55}$$

In the presence of noise and fading, some of the packets are not successfully received. Let p_f denote the probability of failure for a packet in a TDMA scheme. A common approach to deal with the packet loss is to employ an automatic repeat request (ARQ) scheme, by which the receiver requests retransmission of a failed packet. The average number of retransmissions required to ensure a packet is successfully received is $\frac{1}{1-p_f}$. These retransmissions extend the overall collection interval and require extra transmission energy. Following the outage model, the probability of a failed reception is defined as

$$p_f = \text{Prob} \left\{ \frac{X_0}{N_0 B} < b \right\} \tag{56}$$

In a Rayleigh fading channel, this probability is given by

$$p_f = 1 - e^{-b/\gamma_0} \tag{57}$$

The bandwidth and energy requirements of the benchmark network using ARQ now increase as

$$B_{s,ARQ} = \frac{NL}{T(1 - p_f)} = \frac{NLe^{b/\gamma_0}}{T} \tag{58}$$

and

$$E_{ARQ} = NT_p \frac{P_T}{1 - p_f} = NN_0\gamma_0\eta Le^{b/\gamma_0} \tag{59}$$

Under Rayleigh fading, the saving in energy achieved by RACS, over a benchmark network using ARQ is given by

$$G_E = \frac{E_{ARQ}}{E_{\min}(B)} = \frac{e^{b/\gamma_0}}{\lambda_{1s}T} \tag{60}$$

and the saving in bandwidth is given by

$$G_B = \frac{B_{s,ARQ}}{B_s} = \frac{1}{2\beta e \log \frac{1}{1-\alpha_s/N}}. \tag{61}$$

Note that the ARQ scheme is only one viable option to enable reliable data transmission in a sensor network. To ensure reliability of data transfer, few transport layer protocols are proposed in the literature [25], [26]. Rather than individually analyzing each scheme, we note that subjecting the conventional TDMA network to fading and noise inevitably increases the required bandwidth and energy. Thus, we provide a lower bound on the achievable gains by considering a TDMA network in ideal channel conditions (i.e., no fading and no noise).

The lower bound on savings in energy, $G_{E,\text{low}}$, is given by

$$G_{E,\text{low}} = \frac{E_{TDMA}}{E_{\min}(B)} = \frac{1}{\lambda_{1s}T} \tag{62}$$

and the lower bound on savings in bandwidth, $G_{B,\text{low}}$, is given by

$$G_{B,\text{low}} = \frac{B_{s,TDMA}}{B_s} = \frac{1}{2\beta e^{1+b/\gamma_0} \log \frac{1}{1-\alpha_s/N}} \tag{63}$$

Fig. 10 shows these savings achieved over the benchmark scheme. We notice that considerable gain in energy– on the order of 20 dB– is achievable. Also, we observe a reduction in the required bandwidth,

say 20 fold decrease in the bandwidth for a network of size $N = 4 \times 10^4$.

VII. CONCLUSION

RACS is an integrated sensing and communication architecture that combines the concepts of random channel access and compressed sensing to achieve energy and bandwidth efficiency. To address realistic deployments conditions, we took into consideration the impact of channel fading and noise on the design and performance of a RACS network. We provided analytical expressions for the minimum bandwidth needed to support the RACS network, as well as the bounds on its energy consumption. For the practical range of the SNR, say 15-25 dB, the minimum required bandwidth in a fading channel is lower than in a non-fading channel; however, the energy consumption is higher in fading. More importantly, it was shown that RACS achieves considerable energy and bandwidth gains over a benchmark TDMA network.

In addition to energy and bandwidth efficiency, RACS affords scalability and robustness against random (isolated) node failures, since the loss of a packet at random bears no consequence on the random nature of the packet arrival process. These features constitute an attractive scheme for large scale wireless sensor networks, deployed for long term monitoring of sparse phenomena (e.g., environmental monitoring).

APPENDIX A

The probability distribution of X_0 and I_n are given by f_X and f_I, respectively, where

$$f_I = \begin{cases} f_Y & \text{for } I_n = Y_n \\ f_M & \text{for } I_n = M_n \end{cases} \tag{64}$$

We define two new random variables $\gamma = \frac{X_0}{I_n + N_0 B}$ and $w = I_n + N_0 B$. We have that

$$f_{\gamma,w}(\gamma, w) = f_{X_0, I_n}(\gamma w, w - N_0 B).|J| \tag{65}$$

where J is the Jacobian of the transformation

$$J = \left\| \begin{matrix} \frac{\partial X_0}{\partial \gamma} & \frac{\partial X_0}{\partial w} \\ \frac{\partial I_n}{\partial \gamma} & \frac{\partial I_n}{\partial w} \end{matrix} \right\| \tag{66}$$

The joint probability distribution of γ and w is now given by

$$f_{\gamma,w}(\gamma, w) = f_X(\gamma w) f_I(w - N_0 B) w \tag{67}$$

The pdf of γ is then obtained as

$$f_\gamma(\gamma) = \int_{N_0B}^\infty f_{\gamma,w}(\gamma,w)dw \tag{68}$$

Now averaging $p_{s|n}(\gamma)$ in Eq. (15) over the statistics of γ, we have that

$$p_{s|n} = \begin{cases} \int_{bN_0B}^\infty f_X(x)dx & \text{for } n = 0 \\ \int_b^\infty \int_{N_0B}^\infty f_X(\gamma w) f_I(w - N_0B) w \, dw \, d\gamma & \text{for } n \geq 1 \end{cases} \tag{69}$$

APPENDIX B

The distribution of the power of the received signal X_0 in Ricean fading is a non-central χ^2 with 2 degrees of freedom [27] given by

$$f_X(x) = \frac{1+K}{P_0} \cdot e^{-K - \frac{x(1+K)}{P_0}} \cdot I_0\left[2\sqrt{\frac{xK(1+K)}{P_0}}\right] \tag{70}$$

The pdf of Y_n is a non-central χ^2 random variable with $2n$ degrees of freedom given by

$$f_Y(y) = \left(\frac{1+K}{P_0}\right)^{\frac{n+1}{2}} \left(\frac{y}{nK}\right)^{\frac{n-1}{2}} e^{-nK - \frac{y(1+K)}{P_0}} I_{n-1}\left[2\sqrt{\frac{(1+K)nKy}{P_0}}\right] \tag{71}$$

where $I_{n-1}(\cdot)$ is the $(n-1)$-order modified Bessel function of the first kind. Finally,

$$f_M(z) = n\left(1 - Q_1\left(\sqrt{2K}, \sqrt{\frac{2(1+K)z}{P_0}}\right)\right)^{n-1} \frac{1+K}{P_0} \cdot e^{-K - \frac{z(1+K)}{P_0}} \cdot I_0\left[2\sqrt{\frac{zK(1+K)}{P_0}}\right]. \tag{72}$$

ACKNOWLEDGMENT

REFERENCES

[1] J. K. Hart and K. Martinez, "Environmental sensor networks: A revolution in the earth system science?" *Earth-Science Reviews*, vol. 78, pp. 177–191, 2006.

[2] E. M. Sozer, M. Stojanovic, and J. G. Proakis, "Underwater acoustic networks," *IEEE Journal of Oceanic Engineering*, vol. 25, no. 1, pp. 72–83, January 2000.

[3] G. Werner-Allen, J. Johnson, M. Ruiz, J. Lees, and M. Welsh, "Monitoring volcanic eruptions with a wireless sensor network," in *Second European Workshop on Wireless Sensor Networks (EWSN)*, January 2005.

[4] K. Martinez, P. Padhy, A. Elsaify, G. Zou, A. Riddoch, J. Hart, and H. Ong, "Deploying a sensor network in an extreme environment," in *IEEE International Conference on Sensor Networks, Ubiquitous and Trustworthy Computing (SUTC)*, June 2006.

[5] F. Fazel, M. Fazel, and M. Stojanovic, "Compressed sensing in random access networks with applications to underwater monitoring," *Physical Communication (Elsevier) Journal*.

[6] ——, "Random access compressed sensing for energy-efficient underwater sensor networks," *IEEE Journal on Selected Areas in Communications (JSAC)*, vol. 29, no. 8, Sept. 2011.

[7] E. J. Candes, J. Romberg, and T. Tao, "Robust uncertainty principles: Exact signal reconstruction from highly incomplete frequency information," *IEEE Transactions on Information Theory*, vol. 52, pp. 489–509, March 2006.

[8] E. Candes and J. Romberg, "Sparsity and incoherence in compressive sampling," *Inverse Problems*, vol. 23, pp. 969–985, 2006.

[9] E. J. Candes and M. B. Wakin, "An introduction to compressive sampling," *IEEE Signal Processing Magazine*, pp. 21–30, March 2008.

[10] K. R. Rao, D. N. Kim, and J. J. Hwang, "Nonuniform dft," in *Fast Fourier Transform - Algorithms and Applications*, ser. Signals and Communication Technology. Springer, 2011, pp. 195–234.

[11] E. J. Candes, Y. C. Eldar, D. Needell, and P. Randall, "Compressed sensing with coherent and redundant dictionaries," *Applied and Computational Harmonic Analysis*, vol. 31, no. 1, pp. 59–73, 2010.

[12] F. Fazel, M. Fazel, and M. Stojanovic, "Design of a random access network for compressed sensing," in *Information Theory and Applications (ITA)*, February 2011.

[13] L. G. Roberts, "Aloha packet system with and without slots and capture," *SIGCOMM Comput. Commun. Rev.*, vol. 5, pp. 28–42, April 1975.

[14] M. Schwartz, *Mobile Wireless Communications*. Cambridge University Press, 2005.

[15] J. Linnartz, *Narrowband Land-Mobile Radio Networks*. Artech House, Inc., 1993.

[16] M. Zorzi and S. Pupolin, "Outage probability in multiple access packet radio networks in the presence of fading," *IEEE Transactions on Vehicular Technology*, vol. 43, no. 3, pp. 1–6, August 1994.

[17] M. K. Simon and M. Alouini, *Digital Communication over Fading Channels*. John Wiley & Sons, 2005.

[18] H. Suzuki, "A statistical model for urban radio propagation," *IEEE Transactions on Communications*, vol. COM-25, no. 7, pp. 673–680, July 1977.

[19] F. Fazel, M. Fazel, and M. Stojanovic, "Impact of fading on random access compressed sensing," in *45th Annual Asilomar Conference on Signals, Systems, and Computers*, November 2011.

[20] M. Marsan, G. Hess, and S. Gilbert, "Shadowing variability in an urban land mobile environment at 900 mhz," *Electronics Letters*, vol. 26, no. 10, pp. 646 –648, may 1990.

[21] N. C. Beaulieu, A. A. Abu-Dayya, and P. J. McLane, "Estimating the distribution of a sum of independent lognormal random variables," *IEEE Transactions on Communications*, vol. 43, no. 12, Dec. 1995.

[22] S. C. Schwartz and Y. S. Yeh, "On the distribution function and moments of power sums with log-normal components," *The Bell System Technical Journal*, vol. 61, no. 7, Sept. 1982.

[23] L. F. Fenton, "The sum of log-nomral probability distributions in scatter transmission systems," *IRE Transaction on Communication Systems*, vol. 8, March 1960.

[24] P. Cardieri and T. S. Rappaport, "Statistics of the sum of lognormal variables in wireless communication," in *Vehicular Technology Conference (VTC)*, 2000.

[25] P. R. Pereira, A. Grilo, F. Rocha, M. S. Nunes, A. Casaca, C. Chaudet, P. Almstrom, and M. Johansson, "End-to-end reliability in wireless sensor networks: Survey and research challenges," in *EuroFGI Workshop on IP QoS and Traffic Control*, December 2007.

[26] J. Yick, B. Mukherjee, and D. Ghosal, "Wireless sensor network survey," *Computer Networks*, vol. 52, no. 2292-2330, August 2008.

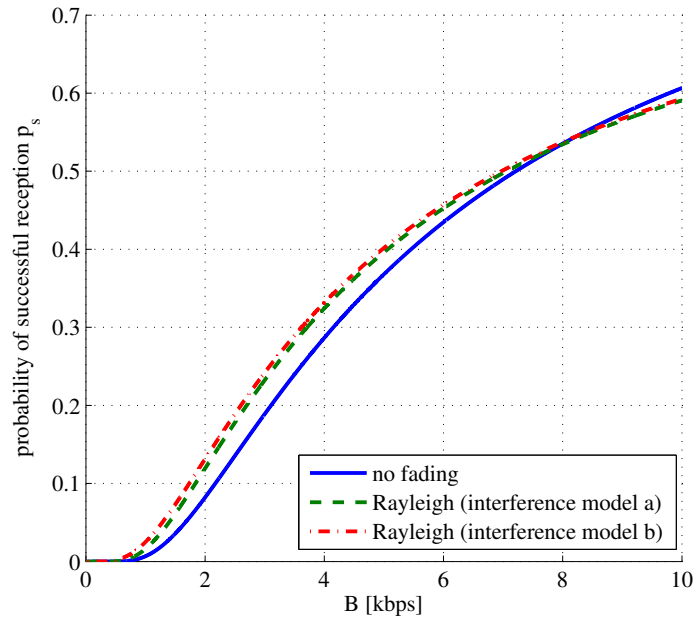[27] J. G. Proakis, *Digital Communications*, 3rd ed. McGraw Hill, 1995.

Fig. 1. Probability of successful reception p_s versus the bandwidth B for a Rayleigh fading channel. Both interference models (a) and (b), corresponding to a lower and an upper bound on the actual p_s are shown. The gap between the two interference models (a) and (b) decreases as bandwidth grows.
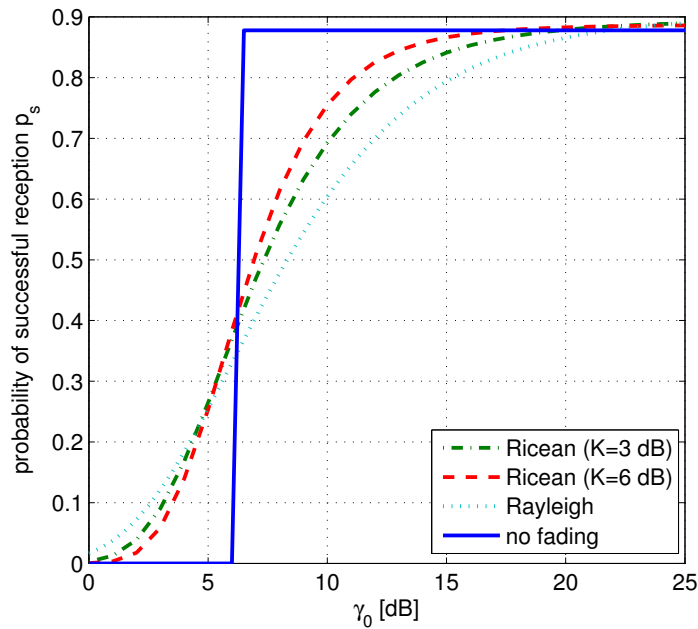

Fig. 2. Probability of successful reception versus γ_0, for $B = 38.4$ kbps over a Ricean fading channel with $K = 3$ and $K = 6$ dB, as well as Rayleigh and non-fading channels. (The value of the bandwidth used corresponds to the Mica2 sensors used in environmental monitoring networks: www.xbow.com).

(a) $\gamma_0 = 15$ dB

(b) $\gamma_0 = 30$ dB
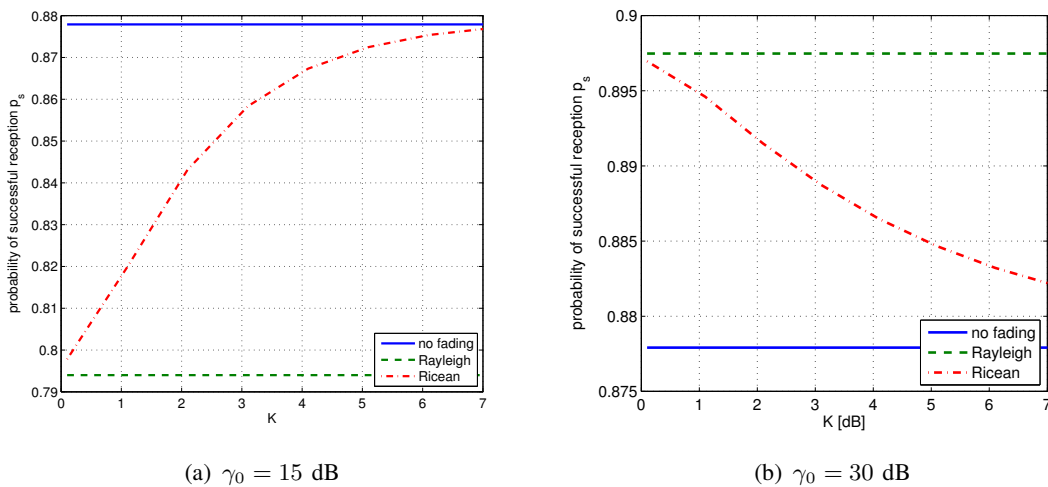
Fig. 3. Probability of successful reception p_s versus the Rice factor K, for $B = 38.4$ kbps. As expected, the Ricean and Rayleigh scenarios converge when $K = 0$, and as K increases, the probability of successful reception in Ricean fading approaches that of the non-fading channel.
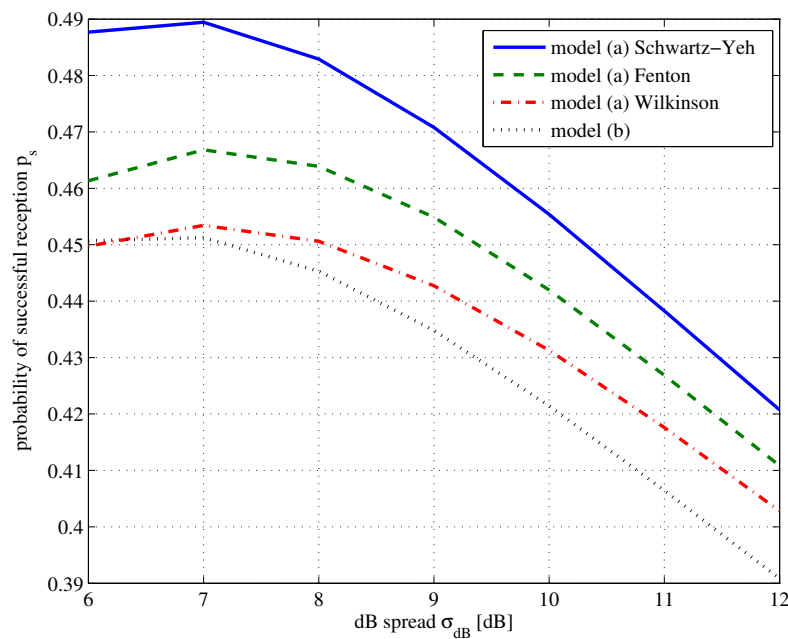
Fig. 4. Probability of successful reception p_s in log-normal shadowing. For interference model (a), Schwartz and Yeh's [22], Fenton's [23] and Wilkinson's [24] methods are considered. We note that compared to our model (b), the approximations used in model (a) do not yield sufficient accuracy to be used in predicting the probability of success. Thus, in case of log-normal shadowing, we abandon model (a) and use model (b) instead.
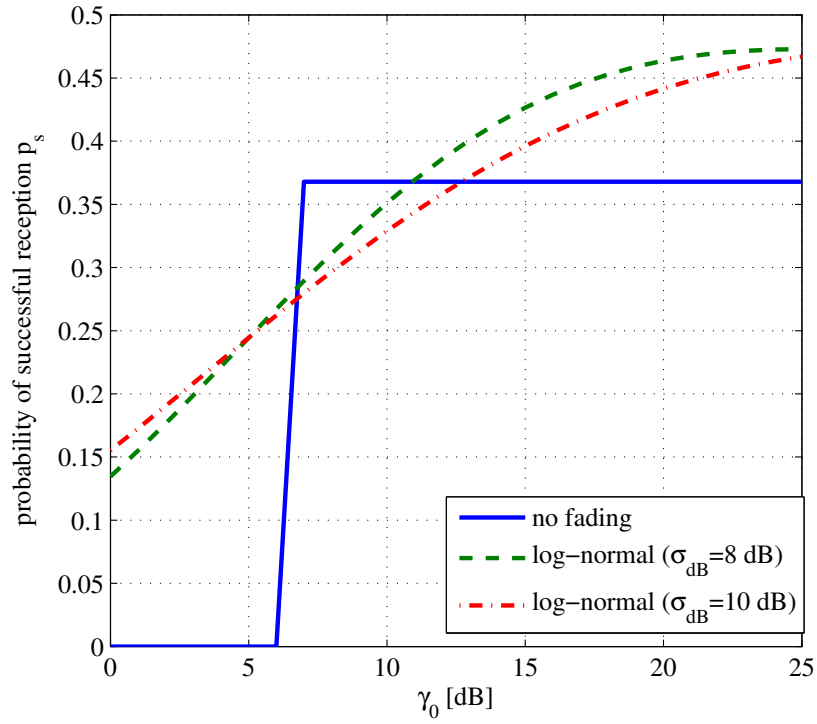
Fig. 5. Probability of successful reception p_s in log-normal shadowing with $B = 5$ kbps. This figure shows that fading improves p_s in both the noise-limited and the interference limited regimes.
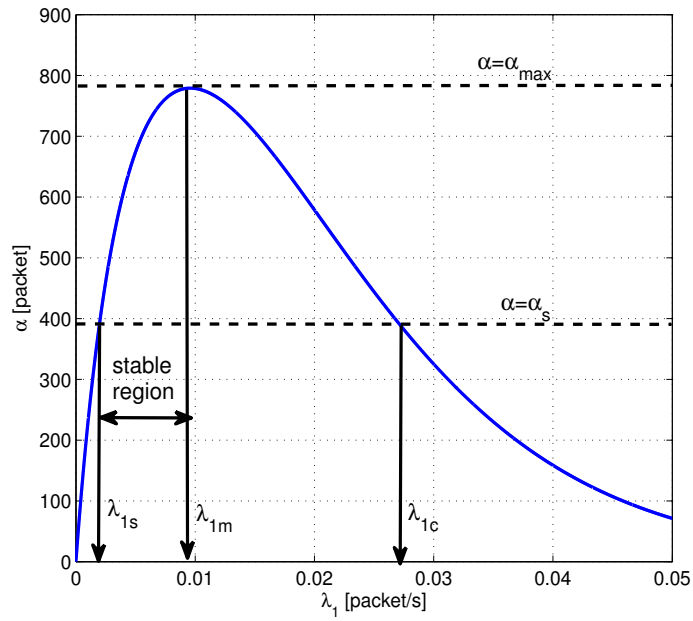

Fig. 6. Average number of useful packets α versus the per-node packet generation rate λ_1. Shown in the figure are λ_{1s} and λ_{1c} (solutions to $\alpha = \alpha_s$) and the region of stability $(\lambda_{1s}, \lambda_{1m})$. Within this region, the desired operating point is near λ_{1s}, which results in the least energy consumption.
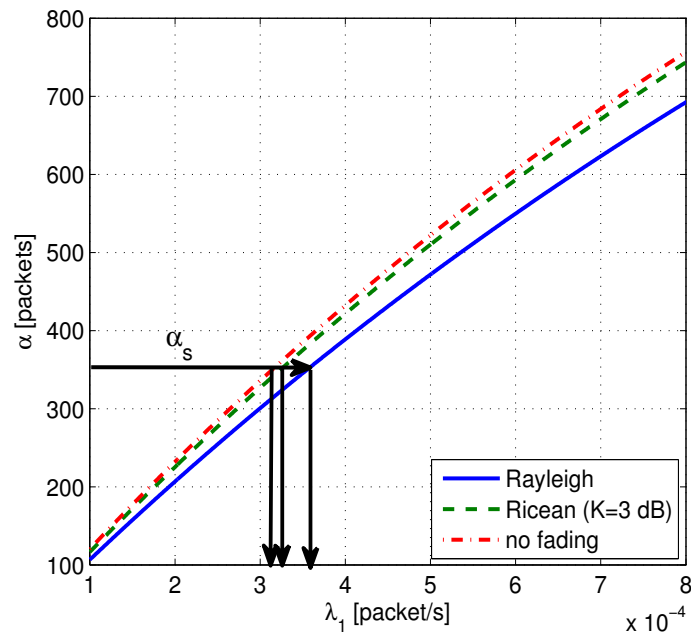
Fig. 7. A required $\alpha_s = 355$ packets, results in a per-node sensing rate $\lambda_{1s} = 3.61 \times 10^{-4}$ for a Rayleigh fading channel, $\lambda_{1s} = 3.3 \times 10^{-4}$ for a Ricean fading channel with $K = 3$ dB, and $\lambda_{1s} = 3.2 \times 10^{-4}$ for a non-fading channel. The rest of the system parameters are $T = 500$ sec, and $B = 38.4$ kbps and $P_s = 0.99$. We notice that for the given parameters the per-node sensing rate is higher in fading.
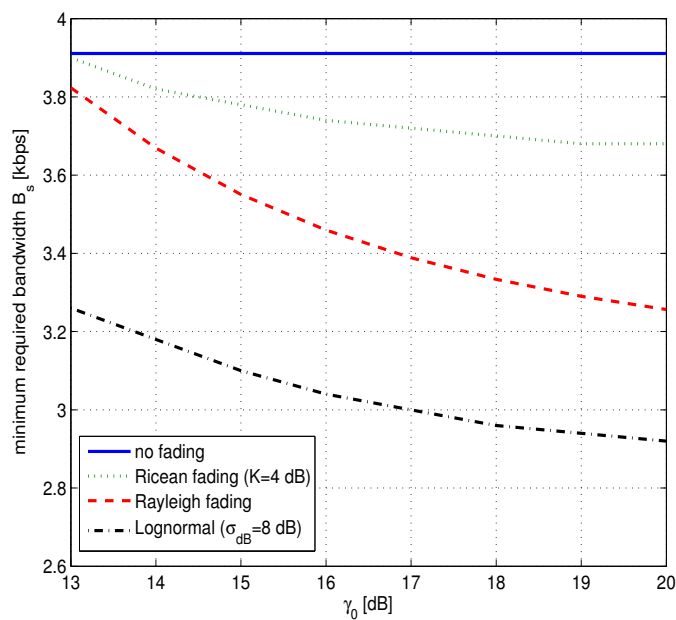

Fig. 8. Minimum bandwidth requirements in Rayleigh, Ricean, Lognormal fading and non-fading channels. System parameters are $T = 500$ sec, $P_s = 0.9$ and $S = 20$. We note that for the moderate and large values of γ_0 fading reduces the required bandwidth.
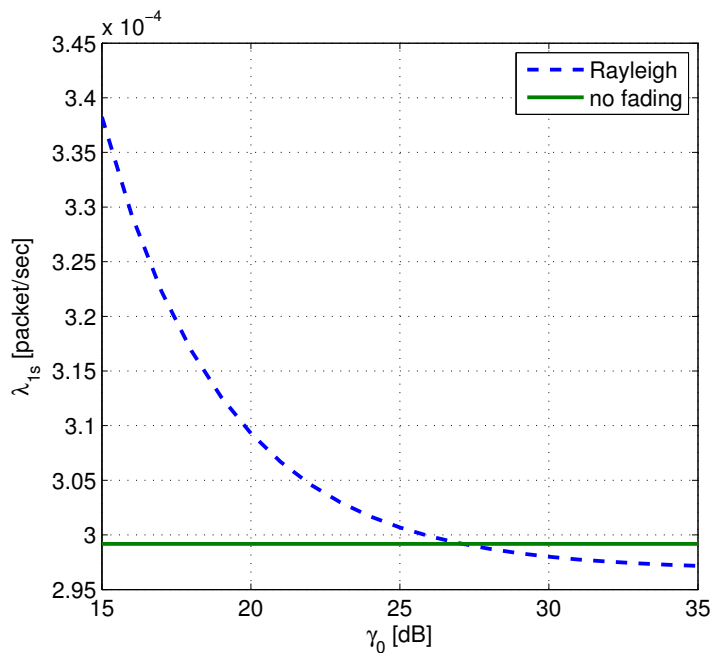
Fig. 9. Minimum required sensing rate λ_{1s} versus γ_0. Increasing γ_0 improves the probability of successful reception in fading (as also observed in Fig. 2) and hence lowers the required sensing rate λ_{1s}. Consequently, in the high-SNR regime, i.e., for $\gamma_0 > 27$ dB, the energy consumption in fading is lower than the energy consumption in non-fading channels.
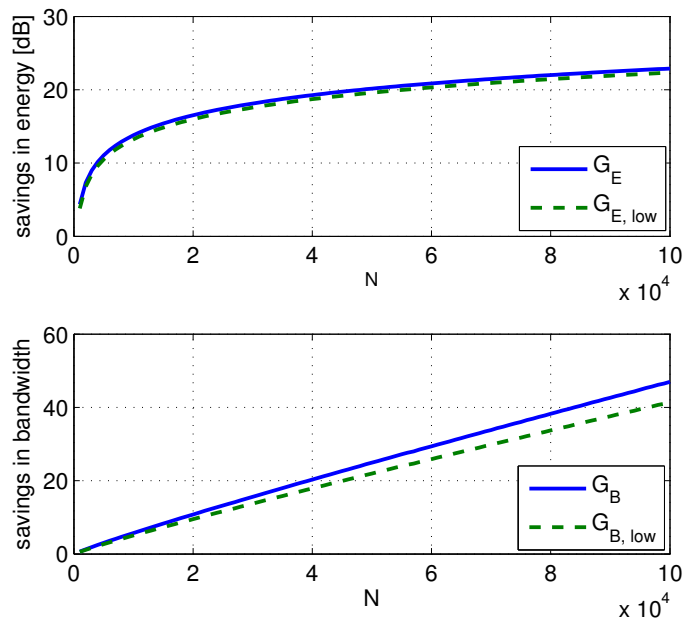

Fig. 10. Savings in energy and bandwidth achieved using RACS (in Rayleigh fading) over a benchmark TDMA scheme. System parameters are $T = 500$ sec, the probability of sufficient sensing $P_s = 0.9$, and $\gamma_0 = 15$ dB. The sparsity is assumed to be fixed at $S = 20$.